ORGANIC CHEMISTRY FRONTIERS

RESEARCH ARTICLE

View Article Online
View Journal | View Issue

Cite this: *Org. Chem. Front.*, 2021, **8**, 5250

A supramolecular dual-donor artificial light-harvesting system with efficient visible light-harvesting capacity†

Yi-Xiong Hu,[a] Pei-Pei Jia,[a] Chang-Wei Zhang,[a] Xing-Dong Xu,*[b] Yanfei Niu,[a] Xiaoli Zhao,[a] Qian Xu,[b] Lin Xu*[a] and Hai-Bo Yang*[a]

Received 21st May 2021,
Accepted 14th July 2021

DOI: 10.1039/d1qo00771h

rsc.li/frontiers-organic

The design and fabrication of highly efficient artificial light-harvesting systems (LHSs) are of great importance in supramolecular chemistry and materials science. Benefitting from the convenient construction process of supramolecular self-assembly, herein, a dual-donor artificial LHS was efficiently constructed through hierarchical self-assembly approaches involving metal–ligand coordination interactions, host–guest interactions and hydrophobic interactions. Notably, compared to the model single-donor artificial LHS with only one donor chromophore, the prepared dual-donor artificial LHS exhibited higher energy transfer efficiency and antenna effects. This research provides an efficient strategy for the construction of artificial LHSs with high energy transfer efficiency and antenna effects.

Introduction

Photosynthesis, a highly efficient process for capturing, transferring, and storing light energy from the sun, exists widely in nature and plays a key role in living systems.[1] As an example, higher plants collect solar energy by a large array of chlorophyll compounds and transform it into chemical energy to produce ATP for vital activities.[2] Inspired by the fascinating function of photosynthesis, much effort in recent decades has been devoted to exploring its complex inner mechanism and mimicking this critical process.[3] To date, a variety of artificial light-harvesting systems (LHSs) benefitting from the primary step of natural photosynthesis for efficiently utilizing light energy have been successfully designed and fabricated for use in photocatalysis and biological imaging.[4]

The critical factors for constructing LHSs include two aspects: (1) multiple donors closely packed around each acceptor without the aggregation-caused quenching (ACQ) phenomenon and (2) a highly efficient energy transfer process based on good spectral overlap between the absorption of the acceptor and the emission of the donor.[5] In recent years, the major developments in the field of artificial LHSs have focused on supramolecular self-assembly involving different weak interactions, owing to their straightforward construction and easily adjustable donor–acceptor ratios compared with those of covalent synthetic methods.[6] For instance, Zhang and Yi recently reported an artificial LHS fabricated using fluorescent metallacycles with highly sequential energy transfer efficiencies and further utilized this LHS for photocatalysis.[7] However, existing reports of artificial LHSs have mainly focused on one type of donor chromophore with narrow absorption, which results in low visible light-harvesting ability compared with plant photosynthesis.[8] Therefore, the development of novel artificial LHSs with improved capacity to harvest visible light has been attracting much attention and is still a great challenge.

Coordination-driven self-assembly, a highly efficient strategy, has been employed to produce discrete supramolecular coordination complexes (SCCs) ranging from two-dimensional metallacycles to three-dimensional metallacages with well-defined topological structures.[9] Due to the metal–ligand bonds being highly directional and comparatively strong, the self-assembling metallacycles and metallacages prepared through coordination interactions are straightforward and nearly quantitative.[10] During the past few decades, these designed and constructed supramolecular coordination architectures have been endowed with a range of functions involving the fields of supramolecular catalysis,[11] information storage,[12] energy transfer,[13] tumour treatment,[14] and supramolecular radicals.[15] Moreover, the coordination-driven self-

[a]*Shanghai Key Laboratory of Green Chemistry and Chemical Processes, School of Chemistry and Molecular Engineering, East China Normal University, Shanghai 200062, P. R. China. E-mail: hbyang@chem.ecnu.edu.cn, lxu@chem.ecnu.edu.cn*
[b]*Key Laboratory of Special Functional Aggregated Materials of Ministry of Education, School of Chemistry and Chemical Engineering, National Engineering Research Center for Colloidal Materials, Shandong University, Jinan, Shandong 250100, P. R. China. E-mail: xuxd@sdu.edu.cn*

†Electronic supplementary information (ESI) available. See DOI: 10.1039/d1qo00771h

assembly strategy allows for precise control over the shape and size of the final construction as well as the distribution and total number of incorporated functional moieties such as fluorophores. Therefore, self-assembled metallacycles and metallacages are advantageous platforms for preparation of artificial light-harvesting systems. For instance, Mukherjee and Stang *et al.* reported fluorescent hexagonal Pt(II) metallacycles as a new platform to fabricate artificial light-harvesting systems.[4e] Zhang and co-workers constructed two tetragonal prismatic platinum(II) cages as the efficient platform for preparing artificial light-harvesting systems.[4g] However, the application of self-assembled metallacycles and metallacages toward light harvesting is in its infancy. It is worth noting that the introduction of other weak interactions into the coordination structures could construct hierarchical self-assembly systems with attractive features and functions.[16] For example, in our group, we reported two metallacycles decorated with both tetraphenylethene (TPE) and pillar[5]arene moieties to successfully construct cross-linked aggregation-induced emission (AIE) supramolecular polymer gels induced by host–guest interactions *via* hierarchical self-assembly.[17] Due to the convenient preparation method and excellent AIE properties, the hierarchical self-assembly system including TPE and pillar[5]arene-containing metallacycles is an advantageous platform that offers fascinating opportunities to fabricate highly efficient supramolecular artificial LHSs. Moreover, the modification of guest molecules with other AIE compounds with broad absorption in the visible-light range could enhance their capacity to harvest visible light.

To achieve this goal, we employed a 120° TPE-containing dipyridyl donor decorated with pillar[5]arene moieties and a 60° diplatinum(II) acceptor to construct a discrete rhomboidal metallacycle *via* coordination-driven self-assembly in nearly quantitative yield (Scheme 1). Notably, in contrast to the dipyridyl ligand, the prepared metallacycle exhibited unique properties of aggregation-induced emission enhancement (AIEE) induced by coordination interactions. In addition, the optical properties of the host–guest complexes of metallacycles with different neutral dinitrile guests have been investigated. By taking advantage of the AIE properties and spherical morphology of the host–guest complexes based on the prepared metallacycle and a 9,10-distyrylanthrance-containing (DSA) dinitrile guest in THF/water (1/9, v/v), a supramolecular artificial LHS was successfully fabricated by adding the hydrophobic fluorescent dye diketopyrrolopyrrole (DPP) as the acceptor chromophore. More importantly, the introduction of a DSA unit for fabricating the dual-donor system of the LHS, with an expanded absorption range from UV to blue light, caused a noticeable improvement in the energy transfer efficiency and the antenna effect compared to that of the LHS with only a TPE-containing metallacycle as the donor.

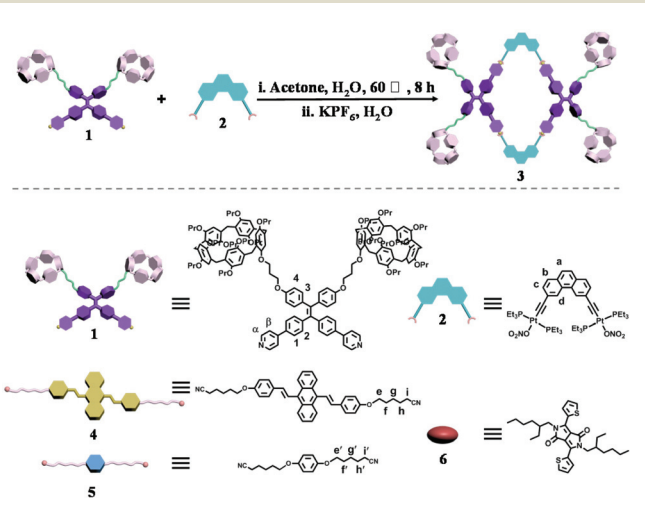

Scheme 1 Self-assembly of 120° dipyridyl donor **1** and 60° diplatinum (II) acceptor **2** into discrete rhomboidal metallacycle **3**, and the chemical structures of building block DSA-containing guest **4**, model guest **5** and fluorescent acceptor **6**.

Results and discussion

Synthesis and characterization

The 120° TPE-containing dipyridyl building block **1** decorated with pillar[5]arene moieties was designed and synthesized as described previously.[17] With the 120° precursor in hand, the self-assembly of a new rhomboidal metallacycle with dual-functional units of TPE and pillar[5]arene was then conducted. Guided by the coordination-driven self-assembly approach, the discrete rhomboidal metallacycle **3** was constructed in quantitative yield by stirring a mixture of 120° donor ligand **1** and 60° diplatinum(II) acceptor **2** at a 1 : 1 molar ratio in acetone/water (5/1, v/v) (Schemes 1 and S1†). The obtained metallacycle **3** was first monitored by $^{31}P\{^{1}H\}$ and ^{1}H multinuclear NMR spectroscopy (Fig. 1a–d).

Multinuclear NMR spectroscopy analysis confirmed that the formed metallacycle had a discrete and highly symmetric structure. For instance, the $^{31}P\{^{1}H\}$ NMR spectra of metallacycle **3** exhibited a sharp singlet at 15.7 ppm, shifted upfield by approximately 4.1 ppm relative to the starting 60° diplatinum(II) acceptor **2**. This upfield shift and the decrease in the coupling of flanking ^{195}Pt satellites *ca.* $\Delta J_{PPt} = -48.5$ Hz for **3** are consistent with back-donation from the platinum atoms. Additionally, significant downfield shifts were observed for metallacycle **3** in the ^{1}H NMR spectra compared to the proton signals of dipyridyl ligand **1**, resulting from the loss of electron density upon the coordination of the Pt(II) metal centre with pyridyl moieties. Moreover, the self-assembly of metallacycle **3** was further studied by 2D NMR techniques (^{1}H–^{1}H COSY, ^{1}H–^{1}H NOESY and DOSY), which proved the successful preparation of rhomboidal metallacycle **3** (Fig. S1–S3†).

ESI-TOF-MS analysis provided further support for the formation of a discrete and highly symmetric metallacycle. As shown in Fig. 1e, the ESI-TOF-MS spectrum of metallacycle **3** exhibited two main peaks at m/z = 2491.13 and 1832.10, corresponding to different charge states owing to the loss of the hexafluorophosphate counterions $[M - 3PF_6^-]^{3+}$ and $[M - 4PF_6^-]^{4+}$, respectively, where M represents the initiating coordi-

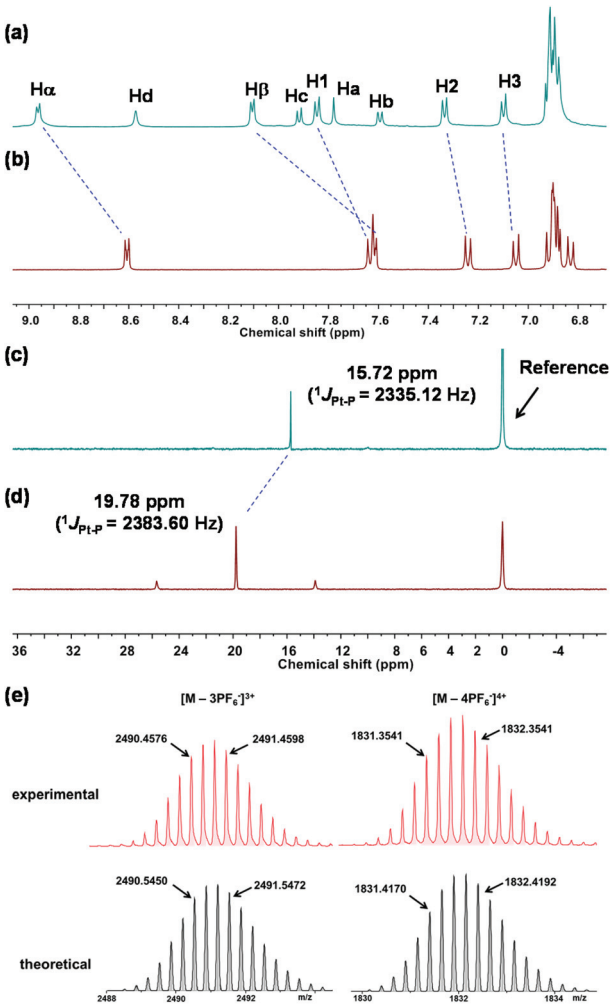

Fig. 1 Partial ^{1}H NMR spectra (500 M, d_6-acetone, 298 K) of rhomboidal metallacycle **3** (a) and 120° dipyridyl donor **1** (b). ^{31}P NMR spectra (202 M, d_6-acetone, 298 K) of rhomboidal metallacycle **3** (c) and 60° diplatinum(II) acceptor **2** (d). Theoretical (*top*) and experimental (*bottom*) ESI-TOF-MS of rhomboidal metallacycle **3**.

nation architecture. More importantly, these peaks were isotopically resolved and were in good agreement with their theoretical distribution, which allowed the structure of the rhomboidal metallacycle **3** to be definitely established.

Pillar[5]arene is capable of binding the neutral dinitrile molecule with strong affinity *via* host–guest interactions in organic solvents, according to previous reports.[18] The driving force of these host–guest processes mainly consists of dipole–dipole forces and [C–H···π], [C–H···N], and [C–H···O] hydrogen bonding. To evaluate the host–guest properties of pillar[5]arene-containing metallacycle **3**, neutral dinitrile guests **4** and **5** with a DSA moiety or a phenyl moiety, respectively, were designed and synthesized (Schemes S2 and S3†). The complexation of metallacycle **3** with dinitrile guest **4** to form complex **3** ⊃ **4** was first investigated by ^{1}H NMR spectroscopy. As indicated in Fig. S4,† the related NMR signals of He–Hi on guest **4** showed obvious broadening and shifted upfield upon the addition of metallacycle **3**. These chemical shift changes of the protons on guest **4** indicated that the electron-rich cavity of pillar[5]arene was successfully threaded by the guest molecule. Moreover, the observation of a distinct band in the 2D DOSY spectrum of the complex of metallacycle **3** and guest **4** indicated the existence of host–guest interactions (Fig. S7†). The host–guest interactions of metallacycle **3** and model guest **5** have also been characterized (Fig. S8–S10†), which proved the successful construction of host–guest complex **3** ⊃ **5**.

Due to the introduction of the TPE units, the AIE properties of ligand **1** and metallacycle **3** were investigated. In this study, THF was employed as a good solvent, and water was selected as a poor solvent. As shown in Fig. 2, metallacycle **3** was emissive even in the original THF solution with a φ_F value of 2.5%, while ligand **1** was non-emissive. This change resulted from the coordination interactions between Pt–N bonds, which restricted the rotation of the phenyl groups on the TPE moieties. With the gradual increase in the water fraction in the THF solution of metallacycle **3**, the emission intensity and fluorescence quantum yield exhibited a dramatic enhancement. The emission intensity of ligand **1** increased slightly when the water fraction was less than 80%. However, a further increase in f_w to 90% significantly enhanced the emission intensity and fluorescence quantum yield of ligand **1**. It should be noted that the fluorescence quantum yield of metallacycle **3** is approximately two times as strong as that of ligand **1**, exhibiting typical AIEE properties induced by metal–ligand coordination interactions. Meanwhile, the AIE properties of DSA-containing guest **4** have also been studied in a mixture of THF and water, as shown in Fig. S12 and S13.† More impor-

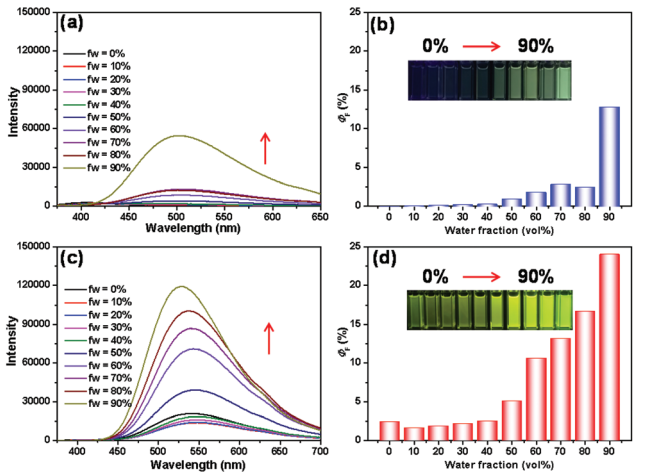

Fig. 2 Fluorescence emission spectra (a) and fluorescence quantum yields (b) of building block **1** *versus* the water fraction in the THF/water mixtures (λ_{ex} = 336 nm; slit widths: ex = 5 nm, em = 5 nm; [TPE unit] = 10 μM). Fluorescence emission spectra (c) and fluorescence quantum yields (d) of rhomboidal metallacycle **3** *versus* the water fraction in the THF/water mixtures (λ_{ex} = 361 nm; slit widths: ex = 5 nm, em = 5 nm; [TPE unit] = 10 μM). Inset: Photographs of building block **1** (b) and rhomboidal metallacycle **3** (d) in THF/water mixtures with different fractions of water upon excitation at 365 nm using an ultraviolet lamp at 298 K ([TPE unit] = 10 μM).

tantly, guest **4** showed an intense absorption band of a peak centred at approximately 415 nm (blue visible light).

Subsequently, with the marriage of TPE-containing metallacycles and DSA-containing dinitrile guests through host–guest interactions, the AIE properties of complex **3** ⊃ **4** were investigated. To enhance the binding ability, the molar ratio of metallacycle **3** and guest compound **4** was adjusted to 1 : 4 to form the complex **3** ⊃ **4**. As shown in Fig. 3a and b, with the gradual increase in the water fractions in the THF solution of complex **3** ⊃ **4**, the emission intensity of the system was gradually enhanced. When the water fraction reached 90%, the obtained fluorescence spectra exhibited the strongest emission intensity, with the fluorescence quantum yield increasing to 21% (Fig. 3e). A similar fluorescence enhancement of the complex **3** ⊃ **5** was observed (Fig. 3c, d and f). These obtained results demonstrated the unique AIE properties of the host–guest complexes of TPE-containing metallacycle **3** with different dinitrile guests.

The sizes and morphologies of the aggregates of host–guest complex **3** ⊃ **4** in THF/water (1 : 9, v/v) were investigated by dynamic light scattering (DLS), scanning electron microscopy (SEM) and transmission electron microscopy (TEM) measurements. A narrow size distribution with an average hydrodynamic diameter of 142 nm was observed by DLS, indicating that the host–guest complex **3** ⊃ **4** forms well-defined nanoaggregates (Fig. 4a). Additionally, the solution exhibited a clear Tyndall effect, as further evidence of the existence of nanoaggregates. TEM and SEM experiments were carried out to determine the morphologies of the aggregates. As shown in Fig. 4b and c, the obtained TEM and SEM images revealed several nearly spherical shapes with an average diameter of approximately 150 nm, which is in agreement with the DLS data. These results combined with the excellent optical properties showed the excellent capability of the aggregates of complex **3** ⊃ **4** in THF/water (1 : 9, v/v) to fabricate artificial LHSs.

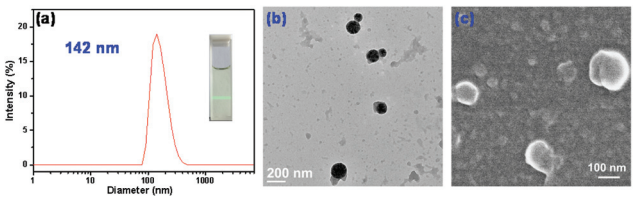

Fig. 4 DLS data (a), TEM image (b) and SEM image (c) of **3** ⊃ **4** in the mixture of THF/water (1 : 9, v/v) ([TPE unit] = 10 μM, [DSA unit] = 20 μM). Inset: Photograph of the Tyndall effect.

To construct LHSs, hydrophobic fluorescent dye **6** (DPP) was chosen as a promising acceptor because its absorption closely matched with the emission of the aggregates of complex **3** ⊃ **4** (Fig. S15†). Then, the light-harvesting behaviour of complex **3** ⊃ **4** and fluorescent dye **6** has been investigated. As shown in Fig. 5b, with the addition of acceptor **6** to the complex **3** ⊃ **4** system, the emission intensity of acceptor **6** at 568 nm gradually increased, accompanied by a decrease in the emission of complex **3** ⊃ **4** at 548 nm when excited at 361 nm. When the ratio of donor **3** ⊃ **4** and acceptor **6** reached 1 : 4 : 0.007, an obvious antenna effect occurred. These observed phenomena suggested that the energy transfer process from **3** ⊃ **4** to **6** effectively took place, and a supramolecular artificial LHS was successfully fabricated. Then, the fluorescence decay profiles were employed to analyse the light-harvesting process. The average fluorescence lifetime (τ) of **3** ⊃ **4** (τ = 2.2 ns) was found to be higher than that of (**3** ⊃ **4**) ⊃ **6** (τ = 1.33 ns), indicating that energy transfer took place from **3** ⊃ **4** to **6** and providing additional evidence that light harvesting was successfully performed. Subsequently, to test the visible light-harvesting property, the absorption of guest **4** at 415 nm was used as the excitation. As shown in Fig. S16,† the fluorescence spectra changed similarly to the excitation at 361 nm, revealing a good artificial LHS with the property of harvesting blue visible light.

In addition, as a control experiment, host–guest complex **3** ⊃ **5** in THF/water (1 : 9, v/v) was used to fabricate artificial LHSs through the addition of acceptor **6** to evaluate the efficiency of the existence of a TPE unit alone with different excitations (361 nm and 415 nm). As shown in Fig. S17a,† with the gradual addition of DPP into the **3** ⊃ **5** system, the starting

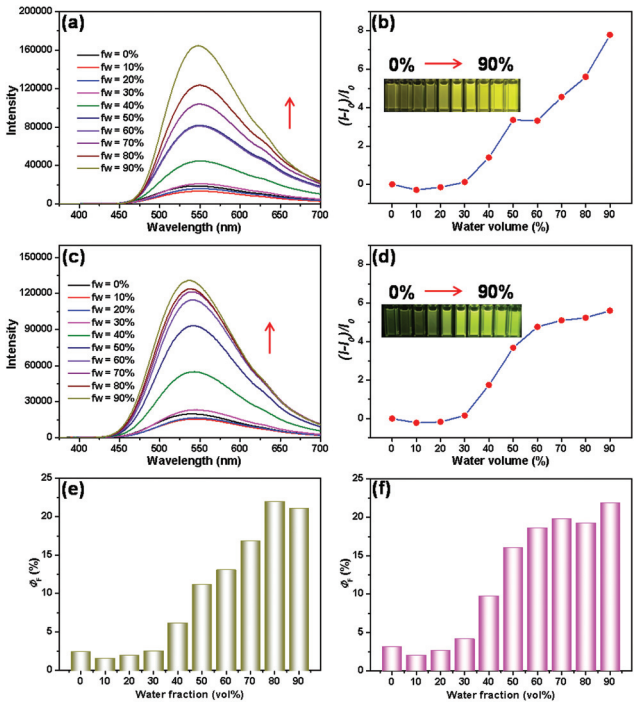

Fig. 3 Fluorescence emission spectra (a) and $(I - I_0)/I_0$ plots (b) of **3** ⊃ **4** *versus* the water fraction in the THF/water mixtures (λ_{em} = 548 nm). Fluorescence emission spectra (c) and plots of $(I - I_0)/I_0$ (d) of **3** ⊃ **5** *versus* the water fraction in the THF/water mixtures (λ_{em} = 537 nm). Fluorescence quantum yields of **3** ⊃ **4** (e) and **3** ⊃ **5** (f) *versus* the water fraction in the THF/water mixtures (λ_{ex} = 361 nm; slit widths: ex = 5 nm, em = 5 nm; [TPE unit] = 10 μM, [DSA unit] = 20 μM, [phenyl unit] = 20 μM). Inset: Photographs of **3** ⊃ **4** (b) and **3** ⊃ **5** (d) in THF/water mixtures with different fractions of water upon excitation at 365 nm using an ultraviolet lamp at 298 K ([TPE unit] = 10 μM, [DSA unit] = 20 μM, [phenyl unit] = 20 μM).

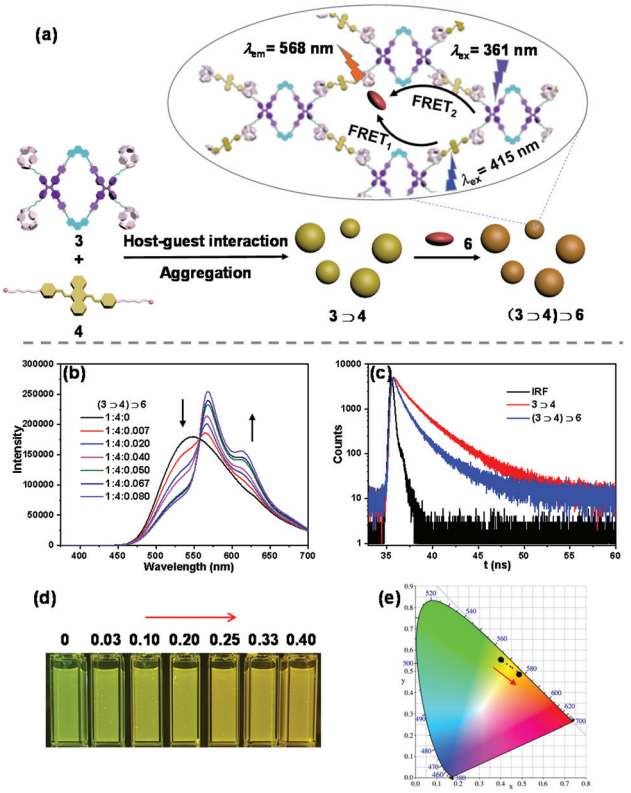

Fig. 5 Scheme of the fabrication of an artificial LHS (a), fluorescence emission spectra of (**3** ⊃ **4**) ⊃ **6** with different concentrations of acceptor **6** (λ_{ex} = 361 nm, slit widths: ex = 5 nm, em = 5 nm) (b), fluorescence decay profiles of **3** ⊃ **4** (1 : 4, red line), and (**3** ⊃ **4**) ⊃ **6** (1 : 4 : 0.08, blue line) (c), photographs of (**3** ⊃ **4**) ⊃ **6** with different concentrations of acceptor **6** upon excitation at 365 nm using an ultraviolet lamp at 298 K (d), fluorescence emission of (**3** ⊃ **4**) ⊃ **6** in the CIE coordinates with different concentrations of acceptor **6** in the mixture of THF/water (1 : 9, v/v) (e). ([TPE unit] = 10 μM, [DSA unit] = 20 μM, [DPP unit] = 0, 0.03, 0.10, 0.20, 0.25, 0.33, 0.40 μM).

emission intensity at 545 nm decreased, while the emission peak at 568 nm ascribed to acceptor **6** gradually increased. According to the fluorescence decay profiles (Fig. S17b†), an obvious decline in the average fluorescence lifetime from **3** ⊃ **5** (τ = 1.82 ns) to (**3** ⊃ **5**) ⊃ **6** (τ = 1.42 ns) was observed. All of the obtained results indicated that the LHS of (**3** ⊃ **5**) ⊃ **6** was successfully fabricated.

To quantitatively evaluate the constructed LHS, the energy transfer efficiency and antenna effect were calculated. According to the fluorescence spectra in Fig. S21 and S23,† the energy transfer efficiency was determined to reach 53.1%, and the antenna effect was estimated to be up to 12.8 for LHS (**3** ⊃ **4**) ⊃ **6** at a ratio of 1 : 4 : 0.08 (excitation at 361 nm). Moreover, as shown in Fig. 6a, after the introduction of DSA units by host–guest interactions to expand the absorption range from UV to blue visible light, the properties of the fabricated LHS were dramatically enhanced. For instance, upon excitation with UV light at 361 nm, the energy transfer efficiency of LHS (**3** ⊃ **4**) ⊃ **6** was calculated to be 1.29-fold as strong as that of the LHS of (**3** ⊃ **5**) ⊃ **6** at a ratio of 1 : 4 : 0.08.

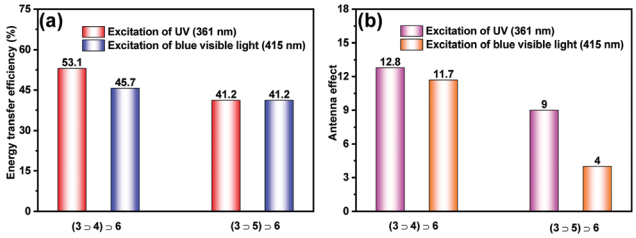

Fig. 6 (a) Energy transfer efficiency and (b) antenna effect of (**3** ⊃ **4**) ⊃ **6** or (**3** ⊃ **5**) ⊃ **6** with different excitations (361 nm and 415 nm) at a ratio of 1 : 4 : 0.08 in the mixture of THF/water (1 : 9, v/v). ([TPE unit] = 10 μM, [DSA unit] = 20 μM, [DPP unit] = 0.4 μM).

It should be noted that the energy transfer efficiency can also be calculated from the time-resolved data.[5a,j] In addition, upon excitation with blue visible light at 415 nm, the antenna effect of LHS (**3** ⊃ **4**) ⊃ **6** was estimated to be approximately 2.9 times to that of (**3** ⊃ **5**) ⊃ **6** (Fig. 6b). These results indicate that the supramolecular artificial LHS (**3** ⊃ **4**) ⊃ **6** could be an efficient platform for harvesting solar energy from the UV and blue visible-light range, which provides a novel strategy to mimic photosynthesis with high energy utilization.

Conclusions

In summary, we successfully developed a dual-donor (TPE-containing metallacycle **3** and DSA-containing dinitrile guest **4**) supramolecular artificial LHS by combining metal–ligand coordination interactions, host–guest interactions and hydrophobic interactions, and it exhibited an excellent capacity for harvesting UV and blue visible light. In comparison with the LHS of the TPE-containing metallacycle **3** alone as the donor, the energy transfer efficiency of the LHS (**3** ⊃ **4**) ⊃ **6** at the ratio of 1 : 4 : 0.08 was enhanced approximately 0.29-fold (excitation at 361 nm), and the antenna effect was enhanced approximately 1.9-fold (excitation at 415 nm). Therefore, this study not only provides a unique strategy for the fabrication of artificial LHSs, but also offers prospects towards utilizing solar energy for potential applications.

Conflicts of interest

There are no conflicts to declare.

Acknowledgements

This work was supported by the National Nature Science Foundation of China (Nos 21871092 and 21602124), the Fundamental Research Funds for the Central Universities, the Natural Science Foundation of Shandong Province (Grant No. ZR2016BQ11), and the Young Scholars Program of Shandong University (2018WLJH40).

References

1 (*a*) G. McDermott, S. M. Prince, A. A. Freer, A. M. Hawthornthwaite-Lawless, M. Z. Papiz, R. J. Cogdell and N. W. Isaacs, Crystal structure of an integral membrane light-harvesting complex from photosynthetic bacteria, *Nature*, 1995, **374**, 517; (*b*) A. Melis, Photosynthesis-to-fuels: from sunlight to hydrogen, isoprene, and botryococcene production, *Energy Environ. Sci.*, 2012, **5**, 5531.

2 (*a*) T. Pullerits and V. Sundström, Photosynthetic light-harvesting pigment–protein complexes: toward understanding how and why, *Acc. Chem. Res.*, 1996, **29**, 381; (*b*) G. D. Scholes, G. R. Fleming, A. Olaya-Castro and R. van Grondelle, Lessons from nature about solar light harvesting, *Nat. Chem.*, 2011, **3**, 763.

3 (*a*) J. Barber, Photosynthetic energy conversion: natural and artificial, *Chem. Soc. Rev.*, 2009, **38**, 185; (*b*) R. Croce and H. van Amerongen, Natural strategies for photosynthetic light harvesting, *Nat. Chem. Biol.*, 2014, **10**, 492; (*c*) T. Mirkovic, E. E. Ostroumov, J. M. Anna, R. van Grondelle, Govindjee and G. D. Scholes, Light absorption and energy transfer in the antenna complexes of photosynthetic organisms, *Chem. Rev.*, 2017, **117**, 249; (*d*) C.-C. You, R. Dobrawa, C. R. Saha-Möller and F. Würthner, Metallosupramolecular Dye Assemblies, *Top. Curr. Chem.*, 2005, **258**, 39.

4 (*a*) Y. Wang, H. Suzuki, J. Xie, O. Tomita, D. J. Martin, M. Higashi, D. Kong, R. Abe and J. Tang, Mimicking natural photosynthesis: solar to renewable H_2 fuel synthesis by Z-scheme water splitting systems, *Chem. Rev.*, 2018, **118**, 5201; (*b*) G. J. Hedley, A. Ruseckas and I. D. Samuel, Light harvesting for organic photovoltaics, *Chem. Rev.*, 2017, **117**, 796; (*c*) M. Hao, G. Sun, M. Zuo, Z. Xu, Y. Chen, X.-Y. Hu and L. Wang, A supramolecular artificial light-harvesting system with two-step sequential energy transfer for photochemical catalysis, *Angew. Chem.*, 2020, **59**, 10095; (*d*) X. Chen, Q. Cao, H. K. Bisoyi, M. Wang, H. Yang and Q. Li, An efficient near-infrared emissive artificial supramolecular light-harvesting system for imaging in the Golgi Apparatus, *Angew. Chem.*, 2020, **59**, 10493; (*e*) K. Acharyya, S. Bhattacharyya, H. Sepehrpour, S. Chakraborty, S. Lu, B. Shi, X. Li, P. S. Mukherjee and P. J. Stang, Self-assembled fluorescent pt(II) metallacycles as artificial light-harvesting systems, *J. Am. Chem. Soc.*, 2019, **141**, 14565; (*f*) A. Kumar, R. Saha and P. S. Mukherjee, Self-assembled metallasupramolecular cages towards light harvesting systems for oxidative cyclization, *Chem. Sci.*, 2021, **12**, 5319; (*g*) Z. Zhang, Z. Zhao, Y. Hou, H. Wang, X. Li, G. He and M. Zhang, Aqueous platinum(II)-cage-based light-harvesting system for photocatalytic cross-coupling hydrogen evolution reaction, *Angew. Chem.*, 2019, **58**, 8862; (*h*) F. Würthner, C.-C. You and C. R. Saha-Möller, Metallosupramolecular squares: from structure to function, *Chem. Soc. Rev.*, 2004, **33**, 133; (*i*) A. Sautter, B. K. Kaletasü, D. G. Schmid, R. Dobrawa, M. Zimine, G. Jung, I. H. M. van Stokkum, L. D. Cola, R. M. Williams and F. Würthner, Ultrafast Energy-Electron Transfer Cascade in a Multichromophoric Light-Harvesting Molecular Square, *J. Am. Chem. Soc.*, 2005, **127**, 6719; (*j*) C.-C. You, C. Hippius, M. Grüne and F. Würthner, Light-Harvesting Metallosupramolecular Squares Composed of Perylene Bisimide Walls and Fluorescent Antenna Dyes, *Chem. – Eur. J.*, 2006, **12**, 7510.

5 (*a*) H.-Q. Peng, L.-Y. Niu, Y.-Z. Chen, L.-Z. Wu, C.-H. Tung and Q.-Z. Yang, Biological applications of supramolecular assemblies designed for excitation energy transfer, *Chem. Rev.*, 2015, **115**, 7502; (*b*) A. J. P. Teunissen, C. Perez-Medina, A. Meijerink and W. J. M. Mulder, Investigating supramolecular systems using Förster resonance energy transfer, *Chem. Soc. Rev.*, 2018, **47**, 7027; (*c*) L. Wu, C. Huang, B. P. Emery, A. C. Sedgwick, S. D. Bull, X. He, H. Tian, J. Yoon, J. L. Sessler and T. D. James, Förster resonance energy transfer (FRET)-based small-molecule sensors and imaging agents, *Chem. Soc. Rev.*, 2020, **49**, 5110; (*d*) G. R. Fleming, G. S. Schlau-Cohen, K. Amarnath and J. Zaks, Design principles of photosynthetic light-harvesting, *Faraday Discuss.*, 2012, **155**, 27; (*e*) R. A. Miller, N. Stephanopoulos, J. M. McFarland, A. S. Rosko, P. L. Geissler and M. B. Francis, Impact of assembly state on the defect tolerance of TMV-based light harvesting arrays, *J. Am. Chem. Soc.*, 2010, **132**, 6068; (*f*) C. V. Kumar and M. R. Duff, DNA-based supramolecular artificial light harvesting complexes, *J. Am. Chem. Soc.*, 2009, **131**, 16024; (*g*) Y.-X. Hu, W.-J. Li, P.-P. Jia, X.-Q. Wang, L. Xu and H.-B. Yang, Supramolecular artificial light-harvesting systems with aggregation-induced emission, *Adv. Opt. Mater.*, 2020, **8**, 2000265; (*h*) T. Xiao, L. Zhang, H. Wu, H. Qian, D. Ren, Z.-Y. Li and X.-Q. Sun, Supramolecular polymer-directed light-harvesting system based on a stepwise energy transfer cascade, *Chem. Commun.*, 2021, **57**, 5782; (*i*) T. Xiao, X. Wei, H. Wu, K. Diao, Z.-Y. Li and X.-Q. Sun, Acetal-based spirocyclic skeleton bridged tetraphenylethylene dimer for light-harvesting in water with ultrahigh antenna effect, *Dyes Pigm.*, 2021, **188**, 109161; (*j*) T. Xiao, H. Wu, G. Sun, K. Diao, X. Wei, Z.-Y. Li, X.-Q. Sun and L. Wang, An efficient artificial light-harvesting system with tunable emission in water constructed from a H-bonded AIE supramolecular polymer and Nile Red, *Chem. Commun.*, 2020, **56**, 12021.

6 (*a*) J.-J. Li, Y. Chen, J. Yu, N. Cheng and Y. Liu, A supramolecular artificial light-harvesting system with an ultrahigh antenna effect, *Adv. Mater.*, 2017, **29**, 1701905; (*b*) S. Guo, Y. Song, Y. He, X.-Y. Hu and L. Wang, Highly efficient artificial light-harvesting systems constructed in aqueous solution based on supramolecular self-assembly, *Angew. Chem., Int. Ed.*, 2018, **57**, 3163; (*c*) L. Xu, Z. Wang, R. Wang, L. Wang, X. He, H. Jiang, H. Tang, D. Cao and B. Z. Tang, A conjugated polymeric supramolecular network with aggregation-induced emission enhancement: an efficient light-harvesting system with an ultrahigh antenna effect, *Angew. Chem.*, 2020, **59**, 9908; (*d*) X.-H. Wang, N. Song, W. Hou, C.-Y. Wang, Y. Wang, J. Tang and Y.-W. Yang, Efficient

aggregation-induced emission manipulated by polymer host materials, *Adv. Mater.*, 2019, **31**, 1903962; (*e*) C. Li, J. Zhang, S. Zhang and Y. Zhao, Efficient light-harvesting systems with tunable emission through controlled precipitation in confined nanospace, *Angew. Chem.*, 2019, **58**, 1643; (*f*) W.-J. Li, X.-Q. Wang, W. Wang, Z. Hu, Y. Ke, H. Jiang, C. He, X. Wang, Y.-X. Hu, P.-P. Jia, P. Yin, J. Chen, H. Sun, Z. Sun, L. Xu and H.-B. Yang, Dynamic artificial light-harvesting systems based on rotaxane dendrimers, *Giant*, 2020, **2**, 100020; (*g*) Y. Li, Y. Dong, L. Cheng, C. Qin, H. Nian, H. Zhang, Y. Yu and L. Cao, Aggregation-induced emission and light-harvesting function of tetraphenylethene-based tetracationic dicyclophane, *J. Am. Chem. Soc.*, 2019, **141**, 8412; (*h*) C.-L. Sun, H.-Q. Peng, L.-Y. Niu, Y.-Z. Chen, L.-Z. Wu, C.-H. Tung and Q.-Z. Yang, Artificial light-harvesting supramolecular polymeric nanoparticles formed by pillar[5]arene-based host–guest interaction, *Chem. Commun.*, 2018, **54**, 1117; (*i*) T. Xiao, W. Zhong, L. Zhou, L. Xu, X.-Q. Sun, R. B. P. Elmes, X.-Y. Hu and L. Wang, Artificial light-harvesting systems fabricated by supramolecular host–guest interactions, *Chin. Chem. Lett.*, 2019, **30**, 31.

7 D. Zhang, W. Yu, S. Li, Y. Xia, X. Li, Y. Li and T. Yi, Artificial light-harvesting metallacycle system with sequential energy transfer for photochemical catalysis, *J. Am. Chem. Soc.*, 2021, **143**, 1313.

8 (*a*) P. D. Frischmann, K. Mahata and F. Würthner, Powering the future of molecular artificial photosynthesis with light-harvesting metallosupramolecular dye assemblies, *Chem. Soc. Rev.*, 2013, **42**, 1847; (*b*) M. Chen and R. E. Blankenship, Expanding the solar spectrum used by photosynthesis, *Trends Plant Sci.*, 2011, **16**, 427; (*c*) V. Balzani, S. Campagna, G. Denti, A. Juris, S. Serroni and M. Venturi, Harvesting sunlight by artificial supramolecular antennae, *Sol. Energy Mater. Sol. Cells*, 1995, **38**, 159; (*d*) R. K. Dubey, D. Inan, S. Sengupta, E. J. R. Sudholter, F. C. Grozema and W. F. Jager, Tunable and highly efficient light-harvesting antenna systems based on 1,7-perylene-3,4,9,10-tetracarboxylic acid derivatives, *Chem. Sci.*, 2016, **7**, 3517; (*e*) W. R. Dichtel, S. Hecht and J. M. J. Fréchet, Functionally layered dendrimers: a new building block and its application to the synthesis of multichromophoric light-harvesting systems, *Org. Lett.*, 2005, **7**, 4451.

9 (*a*) R. Chakrabarty, P. S. Mukherjee and P. J. Stang, Supramolecular coordination: self-Assembly of finite two- and three-dimensional ensembles, *Chem. Rev.*, 2011, **111**, 6810; (*b*) M. Fujita, M. Tominaga, A. Hori and B. Therrien, Coordination assemblies from a pd(II)-cornered square complex, *Acc. Chem. Res.*, 2005, **38**, 369.

10 (*a*) J. M. Lehn, A. Rigault, J. Siegel, J. Harrowfield, B. Chevrier and D. Moras, Spontaneous assembly of double-stranded helicates from oligobipyridine ligands and copper(I) cations: structure of an inorganic double helix, *Proc. Natl. Acad. Sci. U. S. A.*, 1987, **84**, 2565; (*b*) R. S. Forgan, J.-P. Sauvage and J. F. Stoddart, Chemical topology: complex molecular knots, links, and entanglements, *Chem. Rev.*, 2011, **111**, 5434; (*c*) T. A. Bender, M. Morimoto, R. G. Bergman, K. N. Raymond and F. D. Toste, Supramolecular host-selective activation of Iodoarenes by encapsulated organometallics, *J. Am. Chem. Soc.*, 2019, **141**, 1701; (*d*) S. Chakraborty and G. R. Newkome, Terpyridine-based metallosupramolecular constructs: tailored monomers to precise 2D-motifs and 3D-metallocages, *Chem. Soc. Rev.*, 2018, **47**, 3991; (*e*) D. Zhang, T. K. Ronson and J. R. Nitschke, Functional capsules via subcomponent self-assembly, *Acc. Chem. Res.*, 2018, **51**, 2423; (*f*) A. M. Lifschitz, M. S. Rosen, C. M. McGuirk and C. A. Mirkin, Allosteric supramolecular coordination constructs, *J. Am. Chem. Soc.*, 2015, **137**, 7252; (*g*) T. Nakamura, H. Ube, M. Shiro and M. Shionoya, A self-assembled multiporphyrin cage complex through three different zinc(II) center formation under well-balanced aqueous conditions, *Angew. Chem., Int. Ed.*, 2013, **52**, 720; (*h*) S. Pullen and G. H. Clever, Mixed-ligand metal–organic frameworks and heteroleptic coordination cages as multifunctional scaffolds-A comparison, *Acc. Chem. Res.*, 2018, **51**, 3052; (*i*) X. Liu, Y. Qin, J. Zhu, X. Zhao, T. Cheng, Y. Jiang, H. Sun and L. Xu, Acid-induced tunable white light emission based on triphenylamine derivatives, *Chin. Chem. Lett.*, 2021, **32**, 1537; (*j*) Z.-T. Shi, Y.-X. Hu, Z. Hu, Q. Zhang, S.-Y. Chen, M. Chen, J.-J. Yu, G.-Q. Yin, H. Sun, L. Xu, X. Li, B. L. Feringa, H.-B. Yang, H. Tian and D.-H. Qu, Visible-light-driven rotation of molecular motors in discrete supramolecular metallacycles, *J. Am. Chem. Soc.*, 2021, **143**, 442.

11 (*a*) Y. Ueda, H. Ito, D. Fujita and M. Fujita, Permeable self-assembled molecular containers for catalyst isolation enabling two-step cascade reactions, *J. Am. Chem. Soc.*, 2017, **139**, 6090; (*b*) K. Wu, K. Li, S. Chen, Y.-J. Hou, Y.-L. Lu, J.-S. Wang, M.-J. Wei, M. Pan and C.-Y. Su, The redox coupling effect in a photocatalytic ru^{II}-pd^{II} cage with TTF guest as electron relay mediator for visible-light hydrogen-evolving promotion, *Angew. Chem.*, 2020, **59**, 2639; (*c*) L. Zhao, J. Cai, Y. Li, J. Wei and C. Duan, A host–guest approach to combining enzymatic and artificial catalysis for catalyzing biomimetic monooxygenation, *Nat. Commun.*, 2020, **11**, 2903; (*d*) L.-J. Chen, S. Chen, Y. Qin, L. Xu, G.-Q. Yin, J.-L. Zhu, F.-F. Zhu, W. Zheng, X. Li and H.-B. Yang, Construction of porphyrin-containing metallacycle with improved stability and activity within mesoporous carbon, *J. Am. Chem. Soc.*, 2018, **140**, 5049; (*e*) J. Zhu, X. Liu, J. Huang and L. Xu, Our expedition in the construction of fluorescent supramolecular metallacycles, *Chin. Chem. Lett.*, 2019, **30**, 1767.

12 (*a*) Y.-X. Hu, X. Hao, L. Xu, X. Xie, B. Xiong, Z. Hu, H. Sun, G.-Q. Yin, X. Li, H. Peng and H.-B. Yang, Construction of supramolecular liquid-crystalline metallacycles for holographic storage of colored images, *J. Am. Chem. Soc.*, 2020, **142**, 6285; (*b*) Y. Hou, Z. Zhang, S. Lu, J. Yuan, Q. Zhu, W. P. Chen, S. Ling, X. Li, Y. Z. Zheng, K. Zhu and M. Zhang, Highly emissive perylene diimide-based metalla-

cages and their host–guest chemistry for information encryption, *J. Am. Chem. Soc.*, 2020, **142**, 18763; (*c*) P. Howlader, B. Mondal, P. C. Purba, E. Zangrando and P. S. Mukherjee, Self-assembled pd(II) barrels as containers for transient merocyanine form and reverse thermochromism of spiropyran, *J. Am. Chem. Soc.*, 2018, **140**, 7952; (*d*) A. B. Grommet, L. M. Lee and R. Klajn, Molecular photoswitching in confined spaces, *Acc. Chem. Res.*, 2020, **53**, 2600.

13 (*a*) C.-B. Huang, L. Xu, J.-L. Zhu, Y.-X. Wang, B. Sun, X. Li and H.-B. Yang, *J. Am. Chem. Soc.*, 2017, **139**, 9459; (*b*) P.-P. Jia, L. Xu, Y.-X. Hu, W.-J. Li, X.-Q. Wang, Q.-H. Ling, X. Shi, G.-Q. Yin, X. Li, H. Sun, Y. Jiang and H.-B. Yang, *J. Am. Chem. Soc.*, 2021, **143**, 399; (*c*) M. Yamashina, M. M. Sartin, Y. Sei, M. Akita, S. Takeuchi, T. Tahara and M. Yoshizawa, *J. Am. Chem. Soc.*, 2015, **137**, 9266; (*d*) Q. Ling, T. Cheng, S. Tan, J. Huang and L. Xu, *Chin. Chem. Lett.*, 2020, **31**, 2884; (*e*) Z. Zhang, Z. Zhao, L. Wu, S. Lu, S. Ling, G. Li, L. Xu, L. Ma, Y. Hou, X. Wang, X. Li, G. He, K. Wang, B. Zou and M. Zhang, *J. Am. Chem. Soc.*, 2020, **142**, 2592.

14 (*a*) G. Yu, M. Zhang, M. L. Saha, Z. Mao, J. Chen, Y. Yao, Z. Zhou, Y. Liu, C. Gao, F. Huang, X. Chen and P. J. Stang, Antitumor activity of a unique polymer that incorporates a fluorescent self-assembled metallacycle, *J. Am. Chem. Soc.*, 2017, **139**, 15940; (*b*) Y. Qin, L. J. Chen, F. Dong, S. T. Jiang, G. Q. Yin, X. Li, Y. Tian and H. B. Yang, Light-controlled generation of singlet oxygen within a discrete dual-stage metallacycle for cancer therapy, *J. Am. Chem. Soc.*, 2019, **141**, 8943; (*c*) C. Li, P.-P. Jia, Y.-L. Xu, F. Ding, W.-C. Yang, Y. Sun, X.-P. Li, G.-Q. Yin, L. Xu and G.-F. Yang, Photoacoustic imaging-guided chemo-photothermal combinational therapy based on emissive pt(II) metallacycle-loaded biomimic melanin dots, *Sci. China: Chem.*, 2021, **64**, 134.

15 (*a*) K. Nakabayashi, Y. Ozaki, M. Kawano and M. Fujita, A self-assembled spin cage, *Angew. Chem., Int. Ed.*, 2008, **47**, 2046; (*b*) G.-F. Huo, X. Shi, Q. Tu, Y.-X. Hu, G.-Y. Wu, G.-Q. Yin, X. Li, L. Xu, H.-M. Ding and H.-B. Yang, Radical-induced hierarchical self-assembly involving supramolecular coordination complexes in both solution and solid states, *J. Am. Chem. Soc.*, 2019, **141**, 16014; (*c*) W.-L. Jiang, Z. Peng, B. Huang, X.-L. Zhao, D. Sun, X. Shi and H.-B. Yang, *J. Am. Chem. Soc.*, 2021, **143**, 433.

16 (*a*) L.-J. Chen and H.-B. Yang, Construction of stimuli-responsive functional materials via hierarchical self-assembly involving coordination interactions, *Acc. Chem. Res.*, 2018, **51**, 2699; (*b*) W. Zheng, L.-J. Chen, G. Yang, B. Sun, X. Wang, B. Jiang, G.-Q. Yin, L. Zhang, X. Li, M. Liu, G. Chen and H.-B. Yang, Construction of smart supramolecular polymeric hydrogels cross-linked by discrete organoplatinum(II) metallacycles via post-assembly polymerization, *J. Am. Chem. Soc.*, 2016, **138**, 4927; (*c*) C. Lu, M. Zhang, D. Tang, X. Yan, Z. Zhang, Z. Zhou, B. Song, H. Wang, X. Li, S. Yin, H. Sepehrpour and P. J. Stang, Fluorescent metallacage-core supramolecular polymer gel formed by orthogonal metal coordination and host–guest interactions, *J. Am. Chem. Soc.*, 2018, **140**, 7674; (*d*) Y. Tian, X. Yan, M. L. Saha, Z. Niu and P. J. Stang, Hierarchical self-assembly of responsive organoplatinum(II) metallacycle–TMV complexes with turn-On fluorescence, *J. Am. Chem. Soc.*, 2016, **138**, 12033.

17 C.-W. Zhang, B. Ou, S.-T. Jiang, G.-Q. Yin, L.-J. Chen, L. Xu, X. Li and H.-B. Yang, Cross-linked AIE supramolecular polymer gels with multiple stimuli-responsive behaviours constructed by hierarchical self-assembly, *Polym. Chem.*, 2018, **9**, 2021.

18 (*a*) M. Xue, Y. Yang, X. Chi, Z. Zhang and F. Huang, Pillararenes, a new class of macrocycles for supramolecular chemistry, *Acc. Chem. Res.*, 2012, **45**, 1294; (*b*) Z.-Y. Li, Y. Zhang, C.-W. Zhang, L.-J. Chen, C. Wang, H. Tan, Y. Yu, X. Li and H.-B. Yang, Cross-linked supramolecular polymer gels constructed from discrete multi-pillar[5]arene metallacycles and their multiple stimuli-responsive behavior, *J. Am. Chem. Soc.*, 2014, **136**, 8577.